

# Variation in the reference Shields stress for bed load transport in gravel-bed streams and rivers

Erich R. Mueller and John Pitlick

Department of Geography, University of Colorado, Boulder, Colorado, USA

Jonathan M. Nelson

U.S. Geological Survey, Water Resources Division, Denver, Colorado, USA

Received 29 September 2004; revised 5 January 2005; accepted 2 February 2005; published 12 April 2005.

[1] The present study examines variations in the reference shear stress for bed load transport ( $\tau_r$ ) using coupled measurements of flow and bed load transport in 45 gravel-bed streams and rivers. The study streams encompass a wide range in bank-full discharge (1–2600 m<sup>3</sup>/s), average channel gradient (0.0003–0.05), and median surface grain size (0.027–0.21 m). A bed load transport relation was formed for each site by plotting individual values of the dimensionless transport rate  $W^*$  versus the reach-average dimensionless shear stress  $\tau^*$ . The reference dimensionless shear stress  $\tau_r^*$  was then estimated by selecting the value of  $\tau^*$  corresponding to a reference transport rate of  $W^* = 0.002$ . The results indicate that the discharge corresponding to  $\tau_r^*$  averages 67% of the bank-full discharge, with the variation independent of reach-scale morphologic and sediment properties. However, values of  $\tau_r^*$  increase systematically with average channel gradient, ranging from 0.025–0.035 at sites with slopes of 0.001–0.006 to values greater than 0.10 at sites with slopes greater than 0.02. A corresponding relation for the bank-full dimensionless shear stress  $\tau_{bf}^*$  formulated with data from 159 sites in North America and England, mirrors the relation between  $\tau_r^*$  and channel gradient, suggesting that the bank-full channel geometry of gravel- and cobble-bedded streams is adjusted to a relatively constant excess shear stress,  $\tau_{bf}^* - \tau_r^*$ , across a wide range of slopes.

**Citation:** Mueller, E. R., J. Pitlick, and J. M. Nelson (2005), Variation in the reference Shields stress for bed load transport in gravel-bed streams and rivers, *Water Resour. Res.*, 41, W04006, doi:10.1029/2004WR003692.

## 1. Introduction

[2] Estimates of bed load transport are used in the analysis of a wide range of practical and theoretical problems in hydrology, including the specification of environmental maintenance flows; computation of sediment loads; development of numerical models of channel evolution; and assessments of the effects of watershed disturbance and river management. Ideally, transport estimates should be based on field measurements of bed load taken over a range of flows. However, the effort involved in taking such measurements and the uncertainty associated with the data are often quite large, and thus it sometimes becomes necessary to compute transport rates on the basis of an empirical relation. Although the application of a transport relation is conceptually straightforward, this approach has its own set of limitations. Key among the limitations is the specification of a critical dimensionless shear stress (or Shields stress),  $\tau_c^*$ , for incipient motion. Existing data sets indicate that for a given grain size and shear stress, there is at least a threefold range in  $\tau_c^*$  [Buffington and Montgomery, 1997]. Some of the variation in  $\tau_c^*$  is due to differences in measurement methods [Buffington and Montgomery, 1997]; some is due to

changes in bed surface structures and channel morphology [Church *et al.*, 1998]; and some is due to differences in flow properties arising from changes in bed roughness and channel gradient [Ashida and Bayazit, 1973; Bathurst *et al.*, 1987; Graf, 1991; Shvidchenko and Pender, 2000]. Uncertainties in the selection of  $\tau_c^*$  can lead to large errors in computed transport rates because entrainment is a nonlinear function of flow strength; these effects are particularly important in the range of flows slightly above the threshold for motion, where transport rates increase by orders of magnitude for small changes in shear stress.

[3] The present study examines variations in the threshold shear stress for bed load transport in 45 gravel-bed streams and rivers in the western United States and Canada. We use coupled measurements of flow and bed load transport to formulate a series of bed load rating curves, and from these curves estimate the reference Shields stress  $\tau_r^*$ , corresponding to a dimensionless transport rate  $W^* = 0.002$  [Parker *et al.*, 1982]. This approach avoids some of the ambiguity in defining transport thresholds for poorly sorted gravels, which can be entrained over a relatively wide range of shear stress [Milhous, 1973; Diplas, 1987; Ashworth and Ferguson, 1989; Wilcock and McArdeil, 1993; Wathen *et al.*, 1995; Powell *et al.*, 2001; Church and Hassan, 2002]. In the present study the reference transport rate ( $W^* = 0.002$ ) is assumed to represent flows that are just high enough to begin mobilizing sediment from

the armor layer, i.e., bed surface particles larger than sand and granules (>4 mm). We focus on differences in  $\tau_r^*$  associated with changes in channel gradient and relative roughness. As gradient and relative roughness increase, large particles alter the vertical distribution of velocity and fluid momentum, reducing the shear stress available for sediment transport (skin friction). Modeling sediment transport under these conditions requires either a downward adjustment in the total boundary shear stress,  $\tau_o$ , to account for friction losses due to boulders or woody debris (drag-partitioning; see *Wiberg and Smith* [1991]), or an upward adjustment in  $\tau_r$  to reflect changes in the fluid and gravitational forces acting on grains. Flume experiments show that the net effect of changes in flow and bed structure as channel gradient increases is to initiate transport at much higher Shields stresses than is normally assumed [*Ashida and Bayazit*, 1973; *Bathurst et al.*, 1987; *Graf*, 1991; *Tsujimoto*, 1991; *Shvidchenko and Pender*, 2000]. The relation for  $\tau_r^*$  developed here is based on field data from natural streams. We assume that flow measurements taken at the time of bed load sampling include the effects of form drag, averaged over a suitable area of the bed. The change in effective stress due to large roughness elements carries over into observed relations between shear stress and bed load transport. In a graphical sense the primary effect of increased flow resistance is to shift the position of the bed load rating curve toward higher stresses [*Reid and Laronne*, 1995]. Flow resistance typically increases as relative submergence decreases and streams become steeper, smaller, and coarser near their headwaters [*Knighton*, 1998; *Bathurst*, 2002], which will likely have a primary effect on trends in  $\tau_r^*$ . A simple method for estimating  $\tau_r^*$  based on morphologic properties would be straightforward to implement, and the uncertainty in estimated values of  $\tau_r^*$  is perhaps no worse than that generated through a drag-partitioning model. Additional relations for the reference discharge  $Q_r$  and bank-full dimensionless shear stress  $\tau_{bf}^*$  are developed independently to test the hypothesis that channel morphology in gravel-bed rivers is linked consistently to bed load transport thresholds of the surface bed material.

## 2. Methods

[4] Discharge and bed load transport measurements were obtained from published sources listing data for 45 different gravel-bed stream and rivers [*Milhous*, 1973; *Jones and Seitz*, 1980; *Parker et al.*, 1982; *Andrews and Erman*, 1986; *Rankl and Smalley*, 1992; *Smalley et al.*, 1994; *Andrews*, 1994; *Bunte*, 1998; *Andrews*, 2000; *Ryan and Emmett*, 2002; *Church and Hassan*, 2002; *King et al.*, 2004; T. E. Lisle, personal communication, 2004] (Table 1). The streams and rivers used in the analysis were selected for three reasons: (1) The data sets were readily available; (2) the study sites span a wide range in stream size and channel gradient; and (3) tabular summaries of the individual measurements allowed us to plot the observations and evaluate the importance of trends or anomalies within each data set.

[5] The majority (34 of 45) of the study sites are located in mountainous areas of Idaho, 21 of which are underlain by intrusive igneous rocks of the Idaho batholith [*King et al.*, 2004]; the remaining sites are scattered throughout western North America in areas of mixed lithology. Runoff in all but

two of the basins, Oak Creek and Jacoby Creek, is produced by spring snowmelt. The bank-full discharge  $Q_{bf}$  of the streams ranges from 0.6 to 2600 m<sup>3</sup>/s; the reach-average channel gradient  $S$  ranges from 0.0003 to 0.051; and the median grain size  $D_{50}$  of the bed surface ranges from 0.022 to 0.21 m (Table 1). While we have not systematically classified channel form in the study reaches, inference from published descriptions of channel characteristics and photographs suggests that most reaches would be classified as pool-riffle or plane-bed/rapid morphology [*Montgomery and Buffington*, 1997; *Zimmerman and Church*, 2001]. The published descriptions also indicate at least two step-pool reaches (Cat Spur Creek and West Fork Buckhorn Creek), and several reaches contain large immobile boulders from glacial lag deposits or valley walls (notably the Virgin River, Johns Creek, and Little Slate Creek) [*Whiting et al.*, 1999; *Andrews*, 2000].

[6] Estimates of the reference Shields stress  $\tau_r^*$  were computed from bed load rating curves, developed for each site using field measurements of flow and bed load transport rate. Most of the measurements were taken at gauging stations, and thus the stream width  $B$  and the stream depth  $H$  were known at the time of sampling. Where direct measurements of width and depth during the sampling period were unavailable, hydraulic geometry relations were used to approximate  $B$  and  $H$ . The at-a-site hydraulic geometry relations were well constrained with many measurements taken over a range of flows. Estimates of the total boundary shear stress at the time of sampling were calculated by the depth-slope product:

$$\tau = \rho g H S, \quad (1)$$

where  $\rho$  is the density of water and  $g$  is the gravitational acceleration. The values of  $\tau$  used throughout the paper are uncorrected for the effects of form drag, and effort was made to use data only where shear stress was estimated from equation (1) to maintain consistency between streams. Values of the Shields stress were determined by

$$\tau^* = \frac{\tau}{(\rho_s - \rho)gD_{50}}, \quad (2)$$

where  $\rho_s$  is the density of sediment (assumed to be 2.65 g/cm<sup>3</sup>) and  $D_{50}$  is the reported median grain size of the surface bed material. We used the surface  $D_{50}$  to calculate the reference Shields stress, rather than the substrate  $D_{50}$ , because (1) this value is most often measured in the field and thus almost always reported in published studies, and (2) we were interested in studying how longitudinal changes in bed surface texture affect the mobility of the bed load. Coarser percentiles of the surface sediment size distribution (e.g.,  $D_{90}$ ) were reported for 32 streams. In most cases, surface sediment size distributions were measured using several pebble counts of 100 or more particles sampled randomly from the bed surface.

[7] Bank-full channel dimensions were determined in 32 of the streams directly from field measurements; in the remaining 13 streams, bank-full conditions were estimated from the hydraulic geometry relations for the 1.5-year flood, a reasonable approximation for bank-full flow in snowmelt-dominated streams [*Emmett and Wolman*, 2001].

Table 1. Site Data

Study Reach	Reference <sup>a</sup>	$Q_{bf}$ cm <sup>3</sup> /s	$Q_r$ , cms	$B_{bf}$ , m	$H_{bf}$ , m	Slope	$D_{50}$ , m	$D_{50ss}$ m	$D_{90}$ , m	$D_{50}/D_{90}$	$H_{bf}/D_{50}$	$\tau_{bf}^*$	$\tau_r^*$	$q_{tr}$ , kg/m/s
Big Wood River	1	21.9	13.6	12.8	0.89	0.0091	0.119	0.025	0.353	0.34	7.5	0.041	0.031	0.0048
Blackmare Creek	1	4.7	3.3	6.8	0.56	0.0299	0.099	0.021	0.299	0.33	5.7	0.102	0.090	0.018
Boise River	1	167	45.1	59.1	1.38	0.0038	0.074	0.023	0.167	0.44	18.8	0.043	0.021	0.0013
Cat Spur Creek	1	2.4	0.9	5.5	0.45	0.0111	0.027	0.027	0.080	0.34	16.8	0.113	0.082	0.0022
Dollar Creek	1	7.8	3.6	10.8	0.43	0.0146	0.077	0.022	0.224	0.34	5.6	0.050	0.040	0.0036
Fourth of July Creek	1	3.9	2.9	8.2	0.46	0.0202	0.051	0.051	0.137	0.37	9.0	0.110	0.100	0.0078
Hawley Creek	1	1.3	0.7	6.5	0.24	0.0233	0.040	0.24	0.140	0.29	6.0	0.085	0.070	0.0032
Herd Creek	1	5.5	1.1	9.0	0.48	0.0077	0.067	0.067	0.122	0.55	7.2	0.033	0.016	0.00075
Johns Creek	1	49.0	37.1	18.2	1.10	0.0207	0.207	0.035	1.008	0.21	5.3	0.067	0.057	0.030
Johnson Creek	1	39.7	48.8	24.0	1.01	0.004	0.190	0.015	0.430	0.44	5.3	0.013	0.014	0.0029
Little Buckhorn Creek	1	0.6	0.5	4.3	0.30	0.0509	0.081	0.015	0.285	0.28	3.7	0.114	0.103	0.016
Little Slate Creek	1	12.2	14.1	14.2	0.66	0.0268	0.107	0.024	0.360	0.30	6.2	0.100	0.098	0.025
Lochsa River	1	446	376	77.3	2.70	0.0023	0.137	0.026	0.330	0.42	19.7	0.028	0.026	0.0045
Lolo Creek	1	11.8	5.1	12.2	0.99	0.0097	0.068	0.020	0.172	0.40	14.5	0.085	0.053	0.0046
Main Fork Red River	1	9.4	4.8	11.5	0.62	0.0059	0.059	0.018	0.135	0.44	10.6	0.038	0.030	0.0017
Marsh Creek	1	20.8	5.4	14.3	0.84	0.006	0.056	0.036	0.162	0.35	14.9	0.054	0.033	0.0017
Middle Fork Salmon River	1	214	229	61.1	1.43	0.0041	0.146	0.023	0.370	0.39	9.8	0.024	0.025	0.0047
North Fork Clearwater River	1	453	336	84.0	2.78	0.0005	0.095	0.016	0.200	0.40	29.2	0.009	0.008	0.00045
Rapid River	1	17.7	15.0	18.5	0.64	0.0108	0.079	0.016	0.200	0.34	8.1	0.053	0.049	0.0053
Salmon River below Yankee Fork	1	118	83.2	36.3	1.82	0.0034	0.104	0.025	0.396	0.26	17.5	0.036	0.032	0.0041
Salmon River near Obsidian	1	12.7	12.2	10.2	0.80	0.0066	0.061	0.026	0.148	0.41	13.2	0.053	0.055	0.0038
Salmon River near Shoup	1	326	238	85.2	1.85	0.0019	0.096	0.028	0.203	0.47	19.2	0.022	0.019	0.0017
Selway River	1	652	376	89.2	2.54	0.0021	0.186	0.024	0.313	0.59	13.6	0.017	0.014	0.0028
South Fork Payette River	1	86.4	41.8	51.5	0.95	0.004	0.096	0.020	0.237	0.41	9.9	0.024	0.017	0.0014
South Fork Red River	1	7.3	3.6	8.9	0.62	0.0146	0.096	0.025	0.211	0.45	6.4	0.057	0.042	0.0055
South Fork Salmon River	1	70.8	35.3	34.2	1.72	0.0025	0.038	0.025	0.113	0.34	45.2	0.068	0.050	0.0019
Squaw Creek (U.S. Geological Survey)	1	5.1	0.4	11.3	0.44	0.01	0.046	0.029	0.116	0.40	9.7	0.059	0.052	0.0025
Squaw Creek (U.S. Forest Service)	1	0.6	0.4	2.8	0.24	0.024	0.027	0.029	0.074	0.36	8.8	0.128	0.117	0.0038
Thompson Creek	1	2.5	2.0	6.4	0.33	0.0153	0.062	0.043	0.138	0.45	5.4	0.050	0.046	0.0032
Trapper Creek	1	2.6	1.7	5.9	0.40	0.0414	0.085	0.017	0.300	0.28	4.7	0.118	0.100	0.017
Valley Creek	1	24.1	9.2	24.7	0.79	0.004	0.040	0.021	0.132	0.30	19.6	0.048	0.032	0.0010
West Fork Buckhorn Creek	1	5.7	9.4	9.4	0.57	0.032	0.180	0.020	0.750	0.24	3.2	0.061	0.045	0.016
Oak Creek, Oregon	2, 3	3.4	6.1	6.1	0.45	0.01	0.054	0.020	0.116	0.40	8.3	0.051	0.032	0.0016
Virgin River, Utah	4	7.1	7.8	7.8	0.58	0.004	0.025	0.025	0.074	0.36	23.2	0.056	0.039	0.00065
Sagehen Creek, California	5	2.0	4.9	4.9	0.49	0.0115	0.058	0.030	0.172	0.40	8.4	0.054	0.048	0.0031
Snake River near Anatone, Washington	6	2607	7.7	9.4	5.12	0.001	0.054	0.027	0.054	0.40	94.8	0.059	0.040	0.0021
Battle Creek, Wyoming	7	7.8	7.7	9.4	0.51	0.0206	0.080	0.014	0.014	0.35	6.4	0.080	0.080	0.011
East Fork Savory Creek, Wyoming	7	1.4	0.9	5.1	0.40	0.004	0.045	0.003	0.003	0.45	8.9	0.022	0.018	0.00049
Big Sandstone Creek, Wyoming	7	7.1	7.3	12.2	0.40	0.0144	0.060	0.044	0.044	0.44	6.7	0.059	0.059	0.0045
Wind River, Wyoming	8	142	57.9	41.6	1.67	0.001	0.022	0.044	0.044	0.44	75.8	0.046	0.031	0.00038
Clearwater River, Idaho	6	2210	6.2	5.7	5.27	0.0003	0.074	0.018	0.132	0.30	71.2	0.013	0.008	0.00031
St. Louis Creek, Colorado	9	3.4	6.2	3.4	0.37	0.018	0.076	0.041	0.132	0.30	4.9	0.052	0.051	0.0051
Harris Creek, British Columbia	10	19.0	6.2	4.2	0.42	0.013	0.070	0.041	0.132	0.30	5.1	0.059	0.060	0.0024
Little Granite Creek, Wyoming	11	6.0	6.2	0.81	0.42	0.019	0.081	0.041	0.132	0.30	4.9	0.052	0.051	0.0051
Jacoby Creek, California	12	32.6	6.2	0.83	0.83	0.0062	0.040	0.040	0.132	0.30	20.7	0.078	0.026	0.00089

<sup>a</sup>References are 1, King et al. [2004], U.S. Forest Service Boise Adjudication Team Web site; 2, Parker et al. [1982]; 3, Milhous [1973]; 4, Andrews [2000]; 5, Andrews [1994], Andrews and Erman [1986]; 6, Jones and Seitz [1980]; 7, Rankl and Smalley [1992]; 8, Smalley et al. [1994]; 9, Bunte [1998]; 10, Church and Hassam [2002]; 11, Ryan and Emmett [2002]; 12, T. E. Lisle (personal communication, 2004).

[8] Bed load samples from Oak Creek were collected using a vortex sampler, and bed load samples from Harris Creek were collected with pit samplers; all other samples were collected with a 76- or 152-mm Helley-Smith sampler either by wading or it being suspended from a bridge or cableway. The Helley-Smith samples were collected following the procedure recommended by *Emmett* [1981], with approximately 20 verticals per section and a sampling interval of 30–60 s per vertical. The number of width-integrated samples ranged from 25 to 280, with an average of 92, at the various sites where bed load data were analyzed.

[9] We recognize that bed load measurements made with the standard 76-mm Helley-Smith sampler and a sampling period of 60 s per vertical are not likely to yield bed load particles much larger than 32 mm, particularly in streams with very rough beds. However, without independent data, we have no way of assessing the effects of sampling inefficiencies in our analysis. Field tests conducted by the U.S. Geological Survey [*Emmett*, 1980] indicate that the Helley-Smith sampler has a near-perfect trapping efficiency for particles between 0.5 and 16 mm. Subsequent field tests of the sampler point to several potential problems in performance [*Pitlick*, 1988; *Ryan and Porth*, 1999; *Sterling and Church*, 2002; *Bunte et al.*, 2004]. These issues merit further study; however, the principal advantage of the Helley-Smith sampler is that it is widely used, and thus whatever errors are introduced by sampling inefficiencies are somewhat made up for by the large number of samples, which is the case here.

[10] Values of bed load transport rate were reported in various units of total sample weight per time. These values were converted to the common unit of kg/s, and then divided by the sampling width to give the unit bed load transport rate  $q_b$  in kg/m/s. For purposes of comparison, unit transport rates were expressed in terms of the dimensionless transport parameter proposed by *Parker et al.* [1982]:

$$W^* = \frac{(s-1)gq_b}{\rho_s(\tau/\rho)^{1.5}}, \quad (3)$$

where  $s$  is the specific gravity of sediment. In the original formulation, *Parker et al.* [1982] computed individual values of  $W^*$  for 10 size fractions; for this analysis, we computed a single value of  $W^*$  for each bed load measurement, and plotted these values versus the dimensionless shear stress for the surface median grain size  $\tau_{s0}^*$ . The reference dimensionless shear stress  $\tau_r^*$  was then estimated by eye as the value of  $\tau_{s0}^*$ , corresponding to a dimensionless transport rate of  $W^* = 0.002$  [*Parker et al.*, 1982]. When expressed in terms of flux per unit width, the reference value of  $W^*$  equates to reference mass transport rates  $q_{br}$  of 0.03–0.0003 kg/m/s, with a median  $q_{br}$  of 0.0032 kg/m/s (Table 1). In steep streams (e.g., Harris Creek) the reference value represents an upper limit to the observations, whereas in lower-gradient streams (e.g., Selway River), the reference value of  $W^*$  is approximately half the bank-full discharge (Table 1). The relations between  $W^*$  and  $\tau_{s0}^*$  were generally well defined, although there was considerable scatter in some data sets. Figure 1 shows examples of transport relations for six sites reflecting the full range of conditions. The first two examples (Salmon

River and Selway River; Figure 1) are representative of the majority of the study sites, where the data follow a clearly defined trend; selection of  $\tau_r^*$  values in these cases was straightforward. The next two examples (Battle Creek and Rapid River; Figure 1) are representative of sites with substantial variation in transport rates at low flows. The bed load moving at these flows consists primarily of sand overpassing a stable bed surface; higher transport phases associated with partial or complete mobility of surface-layer particles [*Milhous*, 1973; *Jackson and Beschta*, 1982; *Ashworth and Ferguson*, 1989; *Ryan et al.*, 2002] occur at much higher flows. Estimates of  $\tau_r^*$  in these cases were weighted toward measurements near or above the reference transport rate because the transport relation tends to become much more well defined above this point. The last two examples (Johns Creek and Little Slate Creek; Figure 1) represent very steep streams where the majority of transport measurements fall below the reference transport rate of  $W^* = 0.002$ ; six of the 45 study streams fall into this category. The low values of  $W^*$  in these cases reflect relatively high values of  $\tau$  for a given  $q_b$ , which are inversely related in (3). In order to estimate  $\tau_r^*$  for these sites, we fit the data with the surface-based transport relation of *Parker* [1990]:

$$W^* = 0.002(\tau/\tau_r)^{14.2}, \quad (4)$$

where  $\tau$  is the average boundary shear stress and  $\tau_r$  was adjusted to provide the best visual match to the data trend in the  $W^* - \tau^*$  plot. This  $\tau_r$  was then converted to  $\tau_r^*$  using (2). If this relation proved inaccurate, we simply extrapolated by eye the trend of the relation formed by the data upward to the reference value of  $W^* = 0.002$  to estimate  $\tau_r^*$  [after *Wilcock and Crowe*, 2003]. In cases such as this, where there was a large amount of data scatter, we estimated a value of  $\tau_r^*$  corresponding to the approximate midpoint of the observations. For the sites where individual bed load measurements were available (42 of 45), we estimated the uncertainty in the midpoint value by selecting the smallest and largest values of  $\tau^*$  that could reasonably span the data, similar to the technique used by *Wilcock and Crowe* [2003]; some measurements were treated as outliers and are therefore not included in the error estimate.

[11] Values of the reference shear stress for three sites, Oak Creek, Virgin River, and Harris Creek, were taken from published studies [*Parker et al.*, 1982; *Andrews*, 2000; *Church and Hassan*, 2002], with an adjustment for the grain size used (surface versus substrate  $D_{50}$ ). Slightly different reference transport rates were used in these studies to determine  $\tau_r^*$  (either  $W^* = 0.002$  or 0.0025); however, because of the steepness of the transport relations, this difference has very little effect on the value of the reference shear stress.

[12] In order to provide a context for the flow level associated with  $\tau_r^*$ , we used the local at-a-station hydraulic geometry relation to estimate the reference discharge  $Q_r$  corresponding to the reference shear stress. Hydraulic geometry relations were available for 35 streams. To find  $Q_r$ , we assumed  $S = \text{constant}$  with discharge, and used (2) and (1) to back-calculate the flow depth  $H$  corresponding to  $\tau_r^*$ ; we then used the local hydraulic geometry relation to determine the discharge for that depth. For purposes of

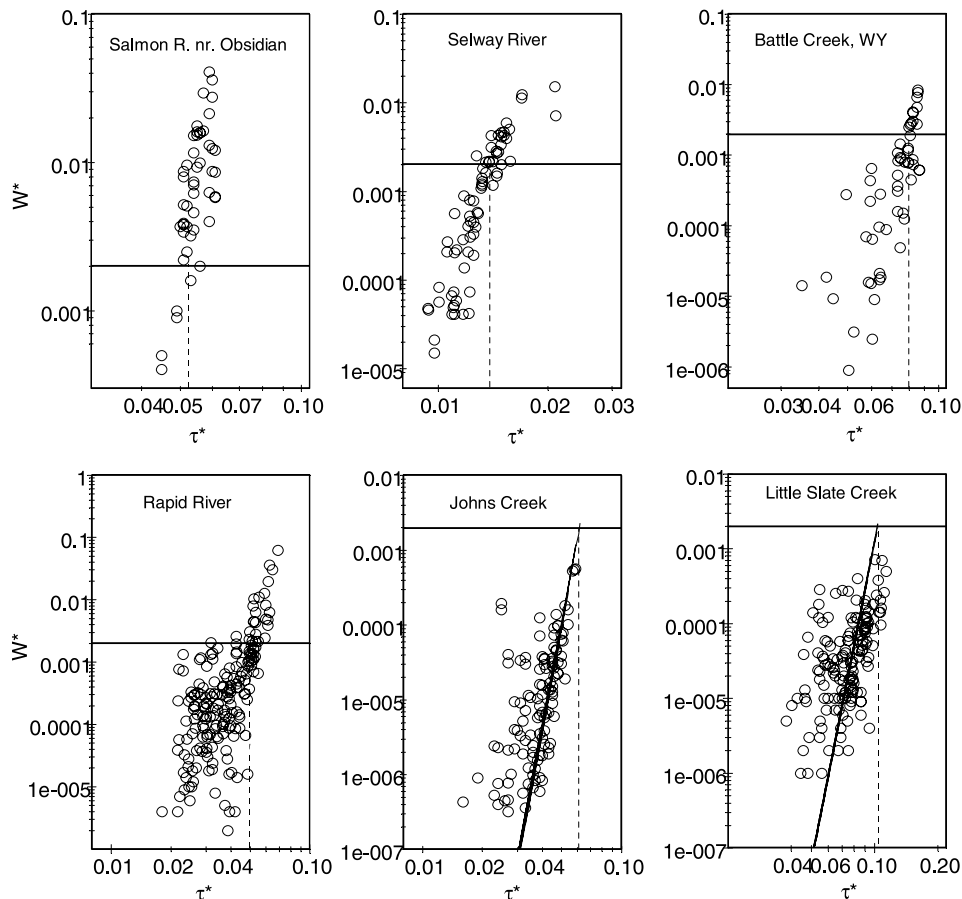


**Figure 1.** Example data sets showing  $\tau_r^*$  versus  $W^*$  used to define reference shear stress for streams of differing data collapse and scatter, as explained in the text.

comparison the values of  $Q_r$  are expressed as a ratio to the bank-full discharge,  $Q_{bf}$ .

### 3. Results

[13] Calculated values of  $\tau_r^*$  vary from about 0.01 to about 0.12, with a median of 0.040 (Table 1). The median value of  $\tau_r^*$  lies in the middle of the range of commonly cited values (0.03–0.06), but the individual estimates appear to vary according to basin size and channel characteristics (Table 1). In general, the values of  $\tau_r^*$  decrease downstream with increasing bank-full discharge,  $Q_{bf}$  (Figure 2a); this trend is clearly associated with downstream increases in flow depths, which lessen the proportion of the total shear stress expended on very large particles. At individual locations,  $\tau_r^*$  ranges from 39 to 109% of the bank-full dimensionless shear stress  $\tau_{bf}^*$ , and on average,  $\tau_r^*$  is about 80% of  $\tau_{bf}^*$  (Table 1). The reference discharge  $Q_r$  ranges from 21 to 123% of  $Q_{bf}$  and averages 67% of  $Q_{bf}$  overall (Figure 2b); the difference between  $Q_r$  and  $Q_{bf}$  does not appear to vary systematically with drainage area, channel gradient, or sediment size. Given the potential practical significance of these results, we wish to clarify this last point: The difference between the values of  $\tau_r^*$  and  $Q_r$ , when expressed as a percentage of bank-full, is not likely the result of random error. The percentage difference between  $\tau_r^*$  and  $Q_r$  arises because the relation between shear stress and discharge is generally nonlinear, with  $\tau^* \propto Q^n$ , and  $n < 1$ . Thus, in general, it requires a relatively large

change in discharge to go from 80% of  $\tau_{bf}^*$  to 100% of  $\tau_{bf}^*$ , which is approximately where we expect the transition from partial transport to complete mobility to occur [see *Pitlick and Van Steeter*, 1998].

[14] Variation in surface  $D_{50}$ , by itself, appears to have little influence on  $\tau_r^*$ . Small mountain streams often have coarse bed material, but several of the data sets used here come from large rivers with relatively coarse bed material (e.g., Selway, Clearwater, and Snake Rivers), which obscures any relation between discharge, grain size, and  $\tau_r^*$ . There is, however, a distinct relation between  $\tau_r^*$  and the range in surface particle sizes at individual localities. Figure 3 plots the calculated values of  $\tau_r^*$  versus the ratio of surface  $D_{50}$  to surface  $D_{90}$  for 32 sites where these data were reported. The relation obtained is statistically significant ( $r^2 = 0.34$ ;  $p < 0.05$ ),

$$\tau_r^* = 0.0086(D_{50}/D_{90})^{-1.57}, \quad (5)$$

and indicates that as the proportion of very coarse particles on the bed surface increases (as the ratio of  $D_{50}$  to  $D_{90}$  decreases),  $\tau_r^*$  generally increases. It appears therefore that coarse particles not only add significantly to the bed roughness, but also enhance the effect of sheltering, which tends to limit the relative mobility of finer particles.

[15] Values of  $\tau_r^*$  were found to be most strongly correlated to average channel gradient  $S$ , bank-full relative depth  $H_{bf}/D_{50}$ , and, ultimately, through the combination of

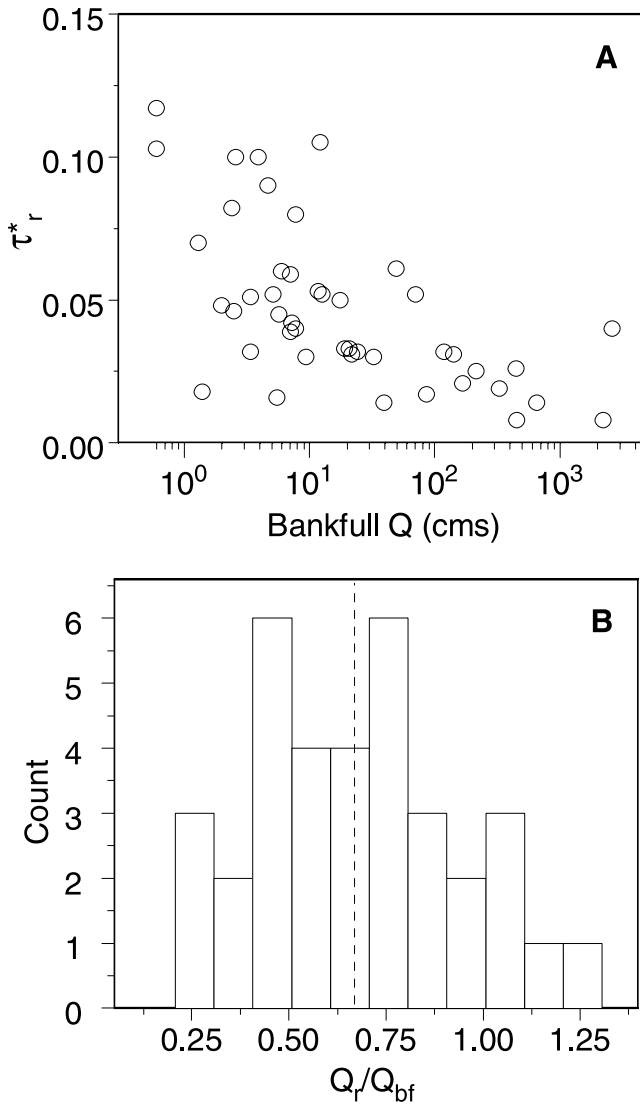


**Figure 2.** (a) The reference Shields stress  $\tau_r^*$  versus bankfull discharge, and (b) histogram of the ratio  $Q_r/Q_{bf}$  with a 0.1 bin size. Vertical dashed line indicates median value.

these factors, to bank-full channel geometry. Figure 4 shows that the calculated values of  $\tau_r^*$  increase systematically with channel gradient; a least squares fit of these data gives the relation

$$\tau_r^* = 2.18S + 0.021, \quad (6)$$

with  $r^2 = 0.70$ ,  $p \ll 0.001$ . Figure 4 also shows error bars associated with individual estimates of  $\tau_r^*$ , spanning the highest and lowest values that could reasonably fit the data. The range in  $\tau_r^*$  appears to increase with channel gradient (Figure 4); however, if the range in  $\tau_r^*$  is expressed in relative terms as a proportion of the median value,  $(\tau_{r-high}^* - \tau_{r-low}^*)/\tau_r^*$ , no trend with slope is evident and the relative range averages 24% for the sites where this could be estimated. It is difficult to determine whether the range in  $\tau_r^*$  is related more to sampling error, sediment supply, or subjectivity in determining the reference Shields stress, but this highlights the importance of carefully choosing appropriate values of  $\tau_r^*$  for sediment transport calculations.

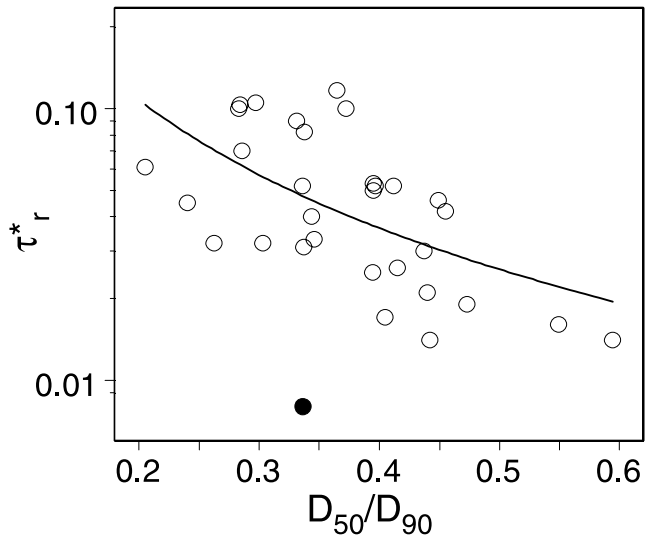


**Figure 3.** Variation in  $\tau_r^*$  with the ratio of  $D_{50}/D_{90}$ . Solid dot is a single outlier.

[16] Figure 5 plots the same data, with the values of  $\tau_r^*$  stratified by bank-full relative submergence  $H_{bf}/D_{50}$ . These data indicate that for a given slope, the estimated values of  $\tau_r^*$  are higher in reaches where  $H_{bf}/D_{50}$  is higher, i.e., where the bed is more submerged (Table 2). While somewhat counterintuitive, this result follows from the proportional relation between bank-full dimensionless shear stress  $\tau_{bf}^*$  and  $(SH_{bf})/D_{50}$ . Thus scatter in the relation for  $\tau_r^*$  is largely attributable to variations in the bank-full  $H/D_{50}$  (Figure 5a), which suggests local adjustment of channel characteristics such that  $\tau_r^*$  increases as  $\tau_{bf}^*$  increases.

[17] As an additional test of the influence of relative submergence, we compiled measurements of grain-size and bank-full channel geometry for 159 gravel-bed streams in North America and Europe [Charlton et al., 1978; Kellerhals et al., 1972; Andrews, 1984; Pitlick and Cress,

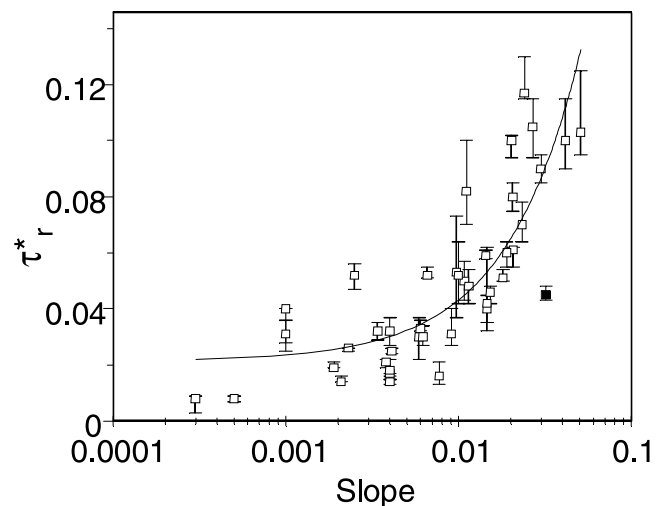


**Figure 4.** Variation in  $\tau_r^*$  as function of slope with error bars indicating range of possible  $\tau_r^*$  values as a characterization of the data scatter. X-axis is in log scale to elucidate individual values. One outlier is shown solid.

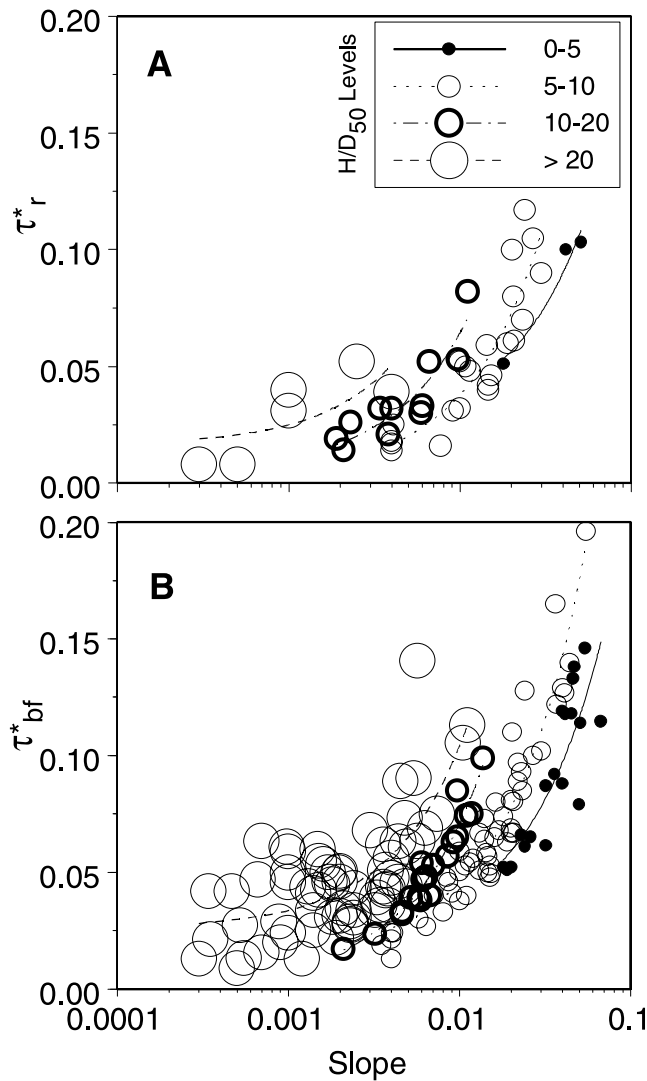


**Figure 5.** The Shields stress  $\tau^*$  versus slope with data stratified by bank-full  $H/D_{50}$ . (a) Values of  $\tau_r^*$  for the bed load data. Jacoby Creek was removed as an outlier. (b) Bank-full  $\tau^*$  for 159 gravel-bed streams in North America and the United Kingdom.

2002; Ryan et al., 2002; Parker et al., 2003; Torizzo and Pitlick, 2004], including those used in this study, and computed individual values of  $\tau_{bf}^*$ . Figure 5b shows that  $\tau_{bf}^*$  varies systematically with channel gradient, and the individual values are likewise stratified by  $H_{bf}/D_{50}$  (as expected). Individual linear regressions were fit to the four categories of  $H_{bf}/D_{50}$ , such that the trend in  $\tau_{bf}^*$  mirrors the one determined for  $\tau_r^*$  for a given category. The slopes of the individual regression equations are very similar (Table 2), especially for the  $H/D_{50}$  categories of 5–10 and 10–20 where the data are well constrained (Figure 5b). The equation describing the overall relation between the bank-full  $\tau^*$  and channel gradient is

$$\tau_{bf}^* = 1.91S + 0.037, \tag{7}$$

with  $r^2 = 0.63$  and  $p \ll 0.001$ .

**Table 2.** Regression Coefficients and Significance for Data as Discussed in the Text<sup>a</sup>

$H/D_{50}$ Level	a	b	$r^2$	p
<i>Reference Shear Stress Data</i>				
0–5	1.68	0.023	0.95	0.15
5–10	3.50	0.0027	0.81	$\ll 0.001$
10–20	5.87	0.0055	0.84	$\ll 0.001$
>20	8.60	0.016	0.46	0.14
All data	2.18	0.021	0.70	$\ll 0.001$
<i>Bank-Full Shear Stress Data</i>				
0–5	1.91	0.021	0.67	$\ll 0.001$
5–10	3.23	0.013	0.90	$\ll 0.001$
10–20	6.83	0.0024	0.93	$\ll 0.001$
>20	7.81	0.026	0.52	$\ll 0.001$
All data	1.91	0.037	0.63	$\ll 0.001$

<sup>a</sup>Variables  $a$  and  $b$  represent the parameters in the relation  $\tau^* = a(S) + b$ .

[18] Figure 6 plots  $\tau_r^*$  versus  $\tau_{bf}^*$  for the 45 streams used in the transport analysis giving the relation

$$\tau_{bf}^* = 1.01\tau_r^* + 0.0099; \tag{8}$$

recall that these values were determined independently. The plot shows that  $\tau_r^*$  and  $\tau_{bf}^*$  are highly correlated ( $r^2 = 0.89$ ;  $p \ll 0.001$ ), and the slope of the relation ( $\sim 1.0$ ) indicates that the difference between  $\tau_{bf}^*$  and  $\tau_r^*$  is essentially constant across the range of study sites. Only one of the 45 sites plots far below the 1:1 line, and on average,  $\tau_{bf}^* - \tau_r^* = 0.010$ . These results imply that streams of almost any size and slope are capable of transporting moderate (and perhaps appreciable) quantities of bed load at bank-full flows. Furthermore, it appears that small steep streams retain their ability to adjust their channel geometry, perhaps

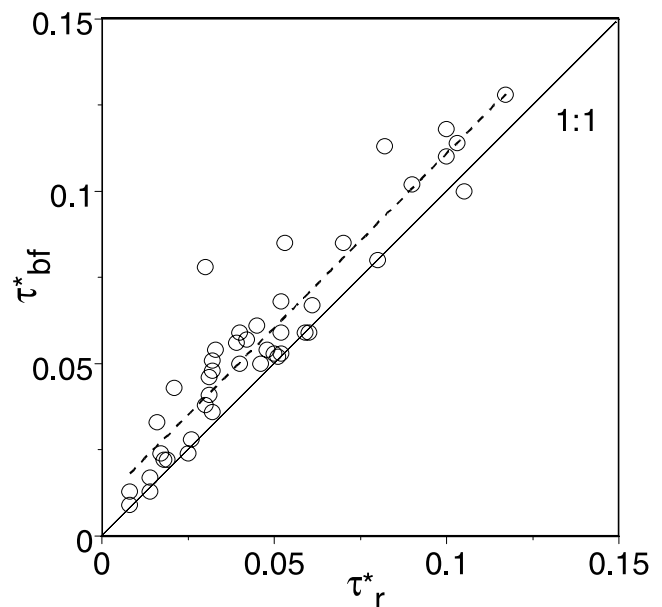


**Figure 6.** Relation between  $\tau_{bf}^*$  and  $\tau_r^*$  for bed load data streams.

very slowly, to maintain consistent values of excess shear stress,  $\tau_{bf}^* - \tau_r^*$ , across a very broad range of scales.

#### 4. Discussion

[19] The results of this analysis indicate that the reference Shields stress for bed load transport  $\tau_r^*$  varies systematically with average channel gradient  $S$  and bank-full relative submergence  $H_{bf}/D_{50}$ . For streams with slopes ranging from 0.001 to 0.006 (typical of gravel-bed rivers), the empirical relation derived here predicts that  $\tau_r^*$  varies from  $\sim 0.025$  to 0.035, bracketing the value of 0.03 that is often cited as a lower limit for bed load transport. For steeper channels, with slopes in the range of 0.02–0.05 (typical of mountain streams),  $\tau_r^*$  increases from the value of 0.06 deduced from the experiments of Shields [1936] to about 0.12. These results, which are based entirely on field data, closely match results obtained in previous experimental studies [Bathurst *et al.*, 1987; Graf, 1991; Buffington and Montgomery, 1997; Shvidchenko and Pender, 2000] and suggest that the processes that drive bed load transport in gravel- and cobble-bed streams change in several important ways as channel gradient increases.

[20] The strong correlation between channel gradient and  $\tau_r^*$  likely relates to several factors. Many of these streams are steep and shallow, and thus some of the stress available for sediment transport is lost as fluid-drag on large particles. Likewise, stabilizing bed structures may develop [Church *et al.*, 1998; Hassan and Church, 2000], increasing the threshold for motion as streams become small near their headwaters. However, the effects of high relative roughness and bed structures do not fully explain the observed trends, particularly in some of the larger channels. Of the 45 streams and rivers used in the analysis, roughly half fall into the category of fully submerged roughness (ratio of bank-full  $H$  to  $D_{90} > 5$ ), yet the values of  $\tau_r^*$  are considerably higher than 0.06. Flume experiments conducted by Shvidchenko and Pender [2000] suggest that the reference shear stress increases systematically with increasing slope, even in flows where the roughness is well submerged. The sediments used by Shvidchenko and Pender [2000] were also very well sorted, and thus any effects associated with form drag or bed structures were presumably absent. At this point we can only suggest that at high slopes there are also changes in flow structure (turbulence) that act independently of changes in sediment texture to alter transport thresholds [see Sumer *et al.*, 2003].

[21] In reviewing the hundreds of transport measurements for the various sites, we could not help but notice that a large proportion of the bed load in these channels consists of sand, even at the highest flows. Furthermore, some of the transport relations are nonstationary or they exhibit seasonal trends (hysteresis) [see Moog and Whiting, 1998; Hassan and Church, 2001]. The predominance of sand in the samples and the nonstationarity of the transport relations suggests that some proportion, perhaps a large proportion, of the bed load is derived from sources other than bed, meaning transport is supply limited. This appears to be the case in Harris Creek, for example, where detailed measurements suggest that the bed load is derived partly from the bed and partly from other sources, such as stream banks and hillslopes [Hassan and Church, 2001; Church and Hassan, 2002]. The data from Rapid River (discussed earlier, Figure 1) likewise exhibit a

wide range in transport rates at flows below the reference value. However, it is also evident in many of the data sets that once  $\tau_r^*$  is reached the transport relation becomes more well defined, presumably because some of the armor-layer particles are beginning to move. Variations in sediment supply and source areas complicate the analysis in some cases, but more often than not, the data converge to form a well-defined trend as transport rates increase.

[22] The observation that sand and granules dominate the bed load of high gradient streams is perhaps not unexpected [Whiting *et al.*, 1999; Habersack and Laronne, 2001; Hassan and Church, 2001; Powell *et al.*, 2001; Rickenmann, 2001]. Particle-size distributions of the subsurface sediment (substrate) given in the various studies used here show that the substrate contains anywhere from 10 to 30% sand. We have collected surface and substrate samples at more than 100 locations on gravel-bed rivers in Colorado and find that the substrate is typically 20–30% sand [Pitlick *et al.*, 2004]. Our data indicate that the substrate in steep headwater reaches is only slightly coarser than the substrate in lower-gradient reaches. In contrast, the bed surface (armor layer) coarsens systematically as slope and shear stress increase. On the basis of the surface layer's appearance, it is natural to assume that the load carried by headwater streams should be relatively coarse; instead, measurements show that the load is mostly sand and granules, suggesting that steep channels are supply limited. We offer a different interpretation, based on the data presented earlier in Figure 3. This figure shows that there is an inverse relation between  $\tau_r^*$  and the ratio of surface  $D_{50}$  to surface  $D_{90}$ , indicating that as the size distribution of the bed surface gets broader,  $\tau_r^*$  increases, and as it gets narrower,  $\tau_r^*$  decreases. If the substrate size distribution is somewhat similar from place to place (as we observe), and if the load is similar in size to the substrate, then sediment moving through a steep headwater reach with a coarse surface layer will be relatively less mobile than sediment moving through a flatter reach with a finer surface layer. Furthermore, the coarse sediment making up the bed surface may be primary in determining flow structure and sediment entrainment, rather than finer particles, and our data imply that the transport thresholds for surface particles are related in a physically consistent way with channel form. We suggest therefore that the effects of high shear stress in steep reaches are more than offset by the effects of hiding and increased flow resistance, such that proportionally higher stresses are required to reach the transport threshold.

[23] While these factors all contribute to variations in transport thresholds, the relation between bank-full  $\tau_r^*$  and reference  $\tau_r^*$  is remarkably consistent over the entire range in channel slope and relative submergence. It appears that in most cases, channel morphology is adjusted such that bank-full flows produce shear stresses slightly above the threshold for local general sediment entrainment. Further, the results of our analysis are consistent with previous results, suggesting that entrainment of gravel making up the bed surface occurs at flows that are, on average, 20–30% less than bank-full flow [Ryan *et al.*, 2002; Whiting and King, 2003].

#### 5. Conclusions

[24] Field measurements from 45 streams in western North America were used to estimate the reference Shields stress  $\tau_r^*$  and reference discharge  $Q_r$  for bed load transport

in natural gravel- and cobble-bed channels. Calculated values of  $\tau_r^*$  were positively correlated to reach-average slope, and stratified by bank-full relative submergence. The analysis indicates that the median  $Q_r$  is 67% of the bank-full flow. In general, flows exceeding this level are expected to produce low to moderate transport rates indicative of entrainment of particles larger than sand and granules. The relation between  $\tau_r^*$  and channel gradient appears applicable to a wide range in stream size and channel slope, especially in snowmelt-dominated gravel-bed streams. The reference  $\tau^*$  was found to be highly correlated to the bank-full  $\tau^*$ , suggesting that the channel morphology of gravel-bed streams and rivers is closely linked to bed load transport thresholds of the surface armor. Because of the sensitivity of bed load transport equations to small variations in excess shear stress, scaling transport relations by an empirically defined reference shear stress, with careful consideration of local channel properties, may increase the accuracy of sediment transport predictions where measurements necessary to estimate the critical shear stress are unavailable.

[25] **Acknowledgments.** The authors would like to thank the U.S. Forest Service Stream Systems Technology Center, particularly John Potyondy and Larry Schmidt, for providing funding for this study; and Tom Lisle and Kristin Bunte for providing useful data sets. We would also like to thank Marwan Hassan and an anonymous reviewer for providing helpful reviews of an earlier version of this manuscript.

## References

- Andrews, E. D. (1984), Bed-material entrainment and hydraulic geometry of gravel-bed rivers in Colorado, *Geol. Soc. Am. Bull.*, 95(3), 371–378.
- Andrews, E. D. (1994), Marginal bed load transport in a gravel bed stream, Sagehen Creek, California, *Water Resour. Res.*, 30(7), 2241–2250.
- Andrews, E. D. (2000), Bed material transport in the Virgin River, Utah, *Water Resour. Res.*, 36, 585–596.
- Andrews, E. D., and D. C. Erman (1986), Persistence in the size distribution of surficial bed material during an extreme snowmelt flood, *Water Resour. Res.*, 22, 191–197.
- Ashida, K., and M. Bayazit (1973), Initiation of motion and roughness of flows in steep channels, in *Proceedings of the 15th Congress, Istanbul, Turkey*, vol. 1, pp. 475–484, Int. Assoc. for Hydraul. Eng. and Res., Madrid.
- Ashworth, P. J., and R. I. Ferguson (1989), Size-selective entrainment of bed load in gravel bed streams, *Water Resour. Res.*, 25, 627–634.
- Bathurst, J. C. (2002), At-a-site variation and minimum flow resistance for mountain rivers, *J. Hydraul. Eng.*, 129, 11–26.
- Bathurst, J. C., H. C. Graf, and H. H. Cao (1987), Bed load discharge equations for steep mountain rivers, in *Sediment Transport in Gravel-Bed Rivers*, edited by C. R. Thorne et al., pp. 453–492, John Wiley, Hoboken, N. J.
- Buffington, J. M., and D. R. Montgomery (1997), A systematic analysis of eight decades of incipient motion studies, with special reference to gravel-bedded rivers, *Water Resour. Res.*, 33, 1993–2029.
- Bunte, K. (1998), Development and field testing of a stationary net-frame bedload sampler for measuring entrainment of pebble and cobble particles, report, 74 pp., Stream Syst. Technol. Cent., Rocky Mt. Res. Stn., U.S. Dep. of Agric. For. Serv., Fort Collins, Colo.
- Bunte, K., S. R. Abt, J. P. Potyondy, and S. E. Ryan (2004), Measurement of coarse gravel and cobble transport using portable bedload traps, *J. Hydraul. Eng.*, 130, 879–893.
- Charlton, F. G., P. M. Brown, and R. W. Benson (1978), The hydraulic geometry of some gravel rivers in Britain, *Rep. IT-180*, Hydraul. Res. Stn., Wallingford, UK.
- Church, M., and M. A. Hassan (2002), Mobility of bed material in Harris Creek, *Water Resour. Res.*, 38, 1237, doi:10.1029/2001WR000753.
- Church, M., M. A. Hassan, and J. F. Wolcott (1998), Stabilizing self-organized structures in gravel-bed streams, *Water Resour. Res.*, 34, 3169–3179.
- Diplas, P. (1987), Bedload transport in gravel-bed streams, *J. Hydraul. Eng.*, 113, 277–292.
- Emmett, W. W. (1980), A field calibration of the sediment-trapping characteristics of the Helley-Smith bedload sampler, *U.S. Geol. Surv. Prof. Pap.*, 1139, 44 pp.
- Emmett, W. W. (1981), Measurement of bed load in rivers, in *Erosion and Sediment Transport Measurement*, IAHS Publ., 133, 3–15.
- Emmett, W. W., and M. G. Wolman (2001), Effective discharge and gravel-bed rivers, *Earth Surf. Processes Landforms*, 26, 1369–1380.
- Graf, W. H. (1991), Flow resistance over a gravel bed: Its consequence on initial sediment movement, in *Fluvial Hydraulics of Mountain Regions*, *Lect. Notes Earth Sci. Ser.*, vol. 37, edited by A. Armanini and G. DiSilvio, pp. 17–32, Springer, New York.
- Habersack, H. M., and J. B. Laronne (2001), Bedload texture in an Alpine gravel bed river, *Water Resour. Res.*, 37, 3359–3370.
- Hassan, M. A., and M. Church (2000), Experiments on surface structure and partial sediment transport on a gravel bed, *Water Resour. Res.*, 36, 1885–1895.
- Hassan, M. A., and M. Church (2001), Rating bed load transport in Harris Creek: Seasonal and spatial variation over a cobble-gravel bed, *Water Resour. Res.*, 37, 813–825.
- Jackson, W. L., and R. L. Beschta (1982), A model of two-phase bedload transport in an Oregon Coast Range stream, *Earth Surf. Processes Landforms*, 7, 517–527.
- Jones, M. L., and H. R. Seitz (1980), Sediment transport in the Snake and Clearwater Rivers in the vicinity of Lewiston, Idaho, *U.S. Geol. Surv. Open File Rep.*, 80-690, 179 pp.
- Kellerhals, R., C. R. Neill, and D. I. Bray (1972), Hydraulic and geomorphic characteristics of rivers in Alberta, *River Eng. Surf. Hydrol. Rep.*, 72-1, Res. Council of Alberta, Edmonton, Canada.
- King, J. G., W. W. Emmett, P. J. Whiting, R. P. Kenworthy, and J. J. Barry (2004), Sediment transport data and related information for selected coarse-bed streams and rivers in Idaho, *Gen. Tech. Rep. RMRS-GTR 131*, 26 pp., Rocky Mt. Res. Stn., U.S. Dep. of Agric. For. Serv., Fort Collins, Colo. (Available at [www.fs.fed.us/rm/boise/teams/soils/Bat%20WWW/index.htm](http://www.fs.fed.us/rm/boise/teams/soils/Bat%20WWW/index.htm).)
- Knighton, A. D. (1998), *Fluvial Forms and Processes—A New Perspective*, 383 pp., Edward Arnold, London.
- Milhous, R. T. (1973), Sediment transport in a gravel-bottomed stream, Ph.D. dissertation, 232 pp., Dep. of Civ. Eng., Oregon State Univ., Corvallis.
- Montgomery, D. R., and J. M. Buffington (1997), Channel-reach morphology in mountain drainage basins, *Geol. Soc. Am. Bull.*, 109(5), 596–611.
- Moog, D. B., and P. J. Whiting (1998), Annual hysteresis in bed load rating curves, *Water Resour. Res.*, 34, 2393–2399.
- Parker, G. (1990), Surface-based bedload transport relation for gravel rivers, *J. Hydraul. Res.*, 28, 417–435.
- Parker, G., P. C. Klingeman, and D. G. McLean (1982), Bedload and size distribution in paved gravel-bed streams, *J. Hydraul. Div. Am. Soc. Civ. Eng.*, 108(HY4), 544–571.
- Parker, G., C. M. Toro-Escobar, M. Ramey, and S. Beck (2003), Effect of floodwater extraction on mountain stream morphology, *J. Hydraul. Eng.*, 129, 887–895.
- Pitlick, J. (1988), Variability of bed load measurement, *Water Resour. Res.*, 24, 173–177.
- Pitlick, J., and R. Cress (2002), Downstream changes in the channel geometry of a large gravel bed river, *Water Resour. Res.*, 38, 1216, doi:10.1029/2001WR000898.
- Pitlick, J., and M. M. Van Steeter (1998), Geomorphology and endangered fish habitats of the upper Colorado River: 2. Linking sediment transport to habitat maintenance, *Water Resour. Res.*, 34, 303–316.
- Pitlick, J., E. Mueller, C. Segura-Sossa, and M. Torizzo (2004), Adjustments of bed sediment texture to variations in shear stress in high gradient streams, *Eos Trans. AGU*, 85(47), Fall Meeting Suppl., Abstract H43A-0363.
- Powell, D. M., I. Reid, and J. B. Laronne (2001), Evolution of bed load grain size distribution with increasing flow strength and the effect of flow duration on the caliber of bed load sediment yield in ephemeral gravel bed rivers, *Water Resour. Res.*, 37, 1463–1474.
- Rankl, J. G., and M. L. Smalley (1992), Transport of sediment by streams in the Sierra Madre, southern Wyoming, *U.S. Geol. Surv. Water Resour. Invest. Rep.*, 92-4091, 36 pp.
- Reid, I., and J. B. Laronne (1995), Bed load sediment transport in an ephemeral stream and a comparison with seasonal and perennial counterparts, *Water Resour. Res.*, 31, 773–781.
- Rickenmann, D. (2001), Comparison of bed load transport in torrents and gravel bed streams, *Water Resour. Res.*, 37, 3295–3305.

- Ryan, S. E., and W. W. Emmett (2002), The nature of flow and sediment movement in Little Granite Creek near Bondurant, Wyoming, *Gen. Tech. Rep. RMRS-GTR-90*, 48 pp., Rocky Mt. Res. Stn., U.S. Dep. of Agric. For. Serv., Fort Collins, Colo.
- Ryan, S. E., and L. S. Porth (1999), A field comparison of three pressure-difference samplers, *Geomorphology*, *30*, 307–322.
- Ryan, S. E., L. S. Porth, and C. A. Troendle (2002), Defining phases of bedload transport using piecewise regression, *Earth Surf. Processes Landforms*, *27*, 971–990.
- Shields, A. (1936), Anwendung der Aehnlichkeitsmechanik und der Turbulenzforschung auf die Geschiebebewegung, *Mitt. Preuss. Versuchsanst. Wasserbau Schiffbau*, *26*, 36 pp.
- Shvidchenko, A. B., and G. Pender (2000), Flume study of the effect of relative depth on the incipient motion of coarse uniform sediments, *Water Resour. Res.*, *36*, 619–628.
- Smalley, M. L., W. W. Emmett, and A. M. Wacker (1994), Annual replenishment of bed material by sediment transport in the Wind River near Riverton, Wyoming, *U.S. Geol. Surv. Water Resour. Invest. Rep.*, *94-40007*, 23 pp.
- Sterling, S., and M. Church (2002), Sediment trapping characteristics of a pit trap and the Helley-Smith sampler in a cobble gravel bed river, *Water Resour. Res.*, *38*, 1144, doi:10.1029/2000WR000052.
- Sumer, B. M., L. H. C. Chua, N. S. Cheng, and J. Fredsoe (2003), Influence of turbulence on bed load sediment transport, *J. Hydraul. Eng.*, *129*, 585–595.
- Torizzo, M., and J. Pitlick (2004), Magnitude-frequency of bed load transport in mountain streams in Colorado, *J. Hydrol.*, *290*, 137–151.
- Tsujimoto, T. (1991), Bed-load transport in steep channels, in *Fluvial Hydraulics of Mountain Regions, Lect. Notes Earth Sci. Ser.*, vol. 37, edited by A. Armanini and G. DiSilvio, pp. 89–102, Springer, New York.
- Wathen, S. J., R. I. Ferguson, T. B. Hoey, and A. Werritty (1995), Unequal mobility of gravel and sand in weakly bimodal river sediments, *Water Resour. Res.*, *31*, 2087–2096.
- Whiting, P. J., and J. G. King (2003), Surface particle sizes on armoured gravel streambeds: Effects of supply and hydraulics, *Earth Surf. Processes Landforms*, *28*, 1459–1471.
- Whiting, P. J., J. F. Stamm, D. B. Moog, and R. L. Orndorff (1999), Sediment-transporting flows in headwater streams, *Geol. Soc. Am. Bull.*, *111*, 450–466.
- Wiberg, P. L., and J. D. Smith (1991), Velocity distribution and bed-roughness in high-gradient streams, *Water Resour. Res.*, *27*, 825–838.
- Wilcock, P. R., and J. C. Crowe (2003), Surface-based transport model for mixed-size sediment, *J. Hydraul. Eng.*, *129*(2), 120–128.
- Wilcock, P. R., and B. W. McArdell (1993), Surface-based fractional transport rates: Mobilization thresholds and partial transport of a sand-gravel sediment, *Water Resour. Res.*, *29*, 1297–1312.
- Zimmerman, A., and M. Church (2001), Channel morphology, gradient profiles and bed stresses during flood in a step-pool channel, *Geomorphology*, *40*, 311–327.

---

E. R. Mueller and J. Pitlick, Department of Geography, University of Colorado, Box 260, Boulder, CO 80309-0260, USA. (erichmueller@hotmail.com)

J. M. Nelson, U.S. Geological Survey, Water Resources Division, Box 25046, Denver Federal Center, Denver, CO 80225, USA.